Atmos. Chem. Phys. Discuss., 15, 29265–29302, 2015
www.atmos-chem-phys-discuss.net/15/29265/2015/
doi:10.5194/acpd-15-29265-2015

Atmospheric Chemistry and Physics Discussions
Open Access

The incorporation of an organic soil layer in the Noah-MP Land Surface Model and its evaluation over a Boreal Aspen Forest

L. Chen[1,2], Y. Li[1], F. Chen[3], A. Barr[4], M. Barlage[3], and B. Wan[3]

[1]Global Institute for Water Security, University of Saskatchewan, Saskatoon, SK, Canada
[2]Key Laboratory of Regional Climate Environment for Temperate East Asia, Institute of Atmospheric Physics, Chinese Academy of Sciences, Beijing, China
[3]National Center for Atmospheric Research, Boulder, Colorado, USA
[4]Environment Canada, National Hydrology Research Center, Saskatoon, SK, Canada

Received: 12 July 2015 – Accepted: 20 October 2015 – Published: 28 October 2015

Correspondence to: Y. Li (yanping.li@usask.ca)

Published by Copernicus Publications on behalf of the European Geosciences Union.

The incorporation of an organic soil layer

L. Chen et al.

Abstract

In this study, the multi-parameterization version of the Noah land-surface model (Noah-MP) was used to investigate the impact of adding a forest-floor organic soil layer on the simulated surface energy and water cycle components at a boreal aspen forest. The test site selected is BERMS Old Aspen Flux (OAS) field station in central Saskatchewan, Canada. The selection of different parameterization schemes for each process within the current Noah-MP model significantly affected the simulation results. The best combination options without incorporating organic soil is referred as the control experiment (CTL). By including an organic-soil parameterization within the Noah-MP model for the first time, the verification results (OGN) against site show significantly improved performance of the model in surface energy fluxes and hydrology simulation due to the lower thermal conductivity and greater porosity of the organic soil. The effects of including an organic soil layer on soil temperature are not uniform throughout the soil depth and year, and those effects are more prominent in summer and in deep soils. For drought years, the OGN simulation substantially modified the partition between direct soil evaporation and vegetation transpiration. For wet years, the OGN simulated latent heat fluxes are similar to CTL except for spring season where OGN produced less evaporation. The impact of the organic soil on sub-surface runoff is substantive with much higher runoff throughout the season.

1 Introduction

Land surface processes play an important role in the climate system by controlling land-atmosphere exchanges of momentum, energy and mass (water, carbon dioxide, and aerosols). Therefore, it is critical to correctly represent these processes in land surface models (LSMs) that are used in weather prediction and climate models (e.g., Dickinson et al., 1986; Sellers et al., 1996; Chen and Dudhia, 2001; Dai et al., 2003; Oleson et al., 2008; Niu et al., 2011). The Noah LSM with multi-parameterization options (Noah-MP) is a new-generation community land model, with multiple options for many land-atmosphere interaction processes representing the seasonal and annual cycles of snow, hydrology, and vegetation (Niu et al., 2011). Noah-MP has been implemented in the community Weather Research and Forecasting (WRF) model (Barlage et al., 2015), the most widely used numerical weather prediction and regional climate model in the world. The performance of Noah-MP was previously evaluated using in-situ and satellite data (Niu et al., 2011; Yang et al., 2011; Cai et al., 2014). Those evaluation results showed, compared to the legacy Noah LSM (Chen et al., 1996; Ek et al., 2003), significant improvements in modeling runoff, snow, surface heat fluxes, soil moisture, and land skin temperature. Recently, Chen et al. (2014) compared Noah-MP to Noah and four other LSMs regarding the simulation of snow and surface heat fluxes at a forested site in the Colorado Headwaters region, and found a generally good performance of Noah-MP. However, it is challenging to parameterize the cascading effects of snow albedo and below-canopy turbulence and radiation transfer in forested regions.

Despite continuous evaluation and improvements, Noah-MP has not been evaluated in boreal forest regions. The Canadian boreal region contains one third of the world's boreal forest, approximately 6 million km^2 (Bryant et al., 1997). The boreal forests have complex interactions with the atmosphere and significant impact on regional and global climate (Bonan, 1991; Bonan et al., 1992; Thomas and Rowntree, 1992; Viterbo and Betts, 1999; Ciais et al., 1995). Several field experiments were conducted to better understand and model these interactions, including BOREAS (Boreal Ecosystem Atmosphere Study) and BERMS (Boreal Ecosystem Research and Monitoring Sites). Numerous studies evaluated LSMs using the BOREAS and BERMS data (Bonan et al., 1997). Levine and Knox (1997) developed a frozen soil temperature (FroST) model to simulate soil moisture and heat flux and used BOREAS northern and southern study areas to calibrate the model. They found that soil temperature was underestimated and large model biases existed when snow was present. Bonan et al. (1997) examined NCAR LSM1 with flux-tower measurements from the BOREAS, and found that the model reasonably simulated the diurnal cycle of the fluxes. Bartlett et al. (2002) used the BOREAS Old Jack Pine (OJP) site to assess two different versions of CLASS, the Canadian Land Scheme (2.7 and 3.0) and found that both versions underestimated the snow depth and soil temperature values, especially the old version CLASS 2.7.

Boreal forest soils often have a relatively thick upper organic horizon. The thickness of the organic horizon directly affects the soil thermal regime and indirectly affects soil hydrological processes. Compared with mineral soil, the thermal and hydraulic properties of the organic soil are significantly different. Dingman (1994) found that the mineral soil porosity ranges from 0.4 to 0.6, while the porosity of organic soil is seldom less than 0.8 (Radforth et al., 1977). The hydraulic conductivity of organic soil horizons can be very high due to the high porosity (Boelter, 1968). Less suction is observed for given volumetric water content in organic soils than in mineral soils except when it reaches saturation. The thermal properties of the soil are also affected by the underground hydrology. Organic soil horizons also have relatively low thermal conductivity, high heat capacity, and a relatively high fraction of plant-available water. Prior studies illustrated the importance of parameterizing organic soil horizons in LSMs for simulating soil temperature and moisture (Letts et al., 2000; Beringer et al., 2001; Molders and Romanovsky, 2006; Nicolsky et al., 2007; Lawrence and Slater, 2008, etc.).

Nevertheless, the current Noah-MP model does not include a parameterization for organic soil horizons. It is thus critical to evaluate the effects of incorporating organic matter on surface energy and water budgets in order to enhance the global applicability of the WRF-Noah-MP coupled modeling system. Here we conducted a detailed examination of the performance of the Noah-MP model in a Canadian boreal forest site. The main objective of this research is to enhance the modeling of vertical heterogeneity (such as organic matter) in soil structures and to understand its impacts on the simulated seasonal and annual cycle of soil moisture and surface heat fluxes. In this paper, we present the BERMS observation site in central Saskatchewan (Sect. 2) used in this study, and our methodology of conducting 12-year Noah-MP simulations with and without organic soil layer for that boreal forest site (Sect. 3). Section 4 dis-

ACPD
15, 29265–29302, 2015

cusses the simulations of the diurnal and annual cycles of the thermal and hydrological components, in dry and wet period separately. Summary and conclusions are given in Sect. 5.

2 Field site and observations

2.1 BERMS site descriptions

The Old Aspen Site (OAS, 53.7° mN, 106.2° W, altitude 601 m) is located in mature deciduous broadleaf forest at the southern edge of the Canadian boreal forest in Prince Albert National Park, Saskatchewan, Canada (Fig. 1). The forest canopy consists of a 22-m trembling aspen overstory (*Populus tremuloides*) with ∼ 10 % balsam poplar (*Populus balsamifera*.) and a 2 m hazelnut understory (*Corylus cornuta*) with sparse alder (*Alnus crispa*). The fully-leafed values of the leaf area index varied among years from 2.0 to 2.9 for the aspen overstory and 1.5 to 2.8 for the hazelnut understory (Barr et al., 2004). The forest regenerated after a natural fire in 1919 and had a 1998 stand density of ∼ 830 stems ha^{-1}. The soil is an Orthic Gray Luvisol with an 8–10 cm deep surface organic Litter layer, Fermentation layer and Humus (LFH) horizon overlying a loam to sandy clay loam mineral soil. 30 % of the fine roots are in the LFH horizon and 60 % are in the upper 20 cm of mineral soil. The water table lies from 1 to 5 m below the ground surface, varying spatially in the hummocky terrain and varying in time in response to variations in precipitation. A small depression near the tower had ponded water at the surface during the wet period from 2005 to 2010. Mean annual air temperature and precipitation at the nearest long-term weather station is 0.4 °C and 467 mm, respectively (Waskesiu Lake, 53°55′ N, 106°04′ W, altitude 532 m, 1971–2000 climatic normal).

Air temperature and humidity were measured at 36-m above ground level using a Vaisala model HMP35cf or HMP45cf temperature/humidity sensor (Vaisala Oyj, Helsinki, Finland) in a 12-plate Gill radiation shield (R.M. Young model 41002-2, Tra-

ACPD
15, 29265–29302, 2015

verse City, MI, USA). Windspeed was measured using a propeller anemometer (R.M. Young model 01503-, Traverse City, MI, USA) located at 38 m above ground level. Atmospheric pressure was measured using a barometer (Setra model SBP270, distributed by Campbell Scientific Inc., Logan, UT, USA). Soil temperature was measured using thermocouples in two profiles at depths of 2, 5, 10, 20, 50 and 100 cm. The two upper measurements were in the forest-floor LFH. Soil volumetric water content was measured using TDR probes (Moisture Point Type B, Gabel Corp., Victoria, Canada) with measurements at depths of 0–15, 15–30, 30–60, 60–90 and 90–120 cm. Three of the eight probes, which were most free of data gaps, were used in this analysis. The TDR probes were located in a low-lying area of the site that was partially flooded after 2004, resulting in high VWC values that may not be characteristic of the flus footprint. θ is also measured at 2.5- and 7.5-cm depth in the forest-floor LFH layer using two profiles of soil moisture reflect meters (model CS615, Campbell Scientific Inc., Logan, UT, USA), inserted horizontally at a location that did not flood.

Eddy-covariance measurements of the sensible and latent heat flux densities were made at 39 m above the ground from a twin scaffold tower. Details of the eddy-covariance systems are given in Barr et al. (2006). Data gaps were filled using a standard procedure.

The net radiation flux density Rn was calculated from component measurements of incoming and outgoing shortwave and longwave radiation, made using paired Kipp and Zonen (Delft, the Netherlands) model CM11 pyranometers and paired Eppley Laboratory (Newport, RI, USA) model PIR pyrgeometers. The upward-facing radiometers were mounted atop the scaffold flux tower in ventilated housings to minimize dew and frost on the sensor domes. The net radiometer and the downward-facing radiometers were mounted on a horizontal boom that extended 4 m to the south of the flux tower, ∼ 10 m above the forest canopy. Details of the minor terms in the surface energy balance; including soil heat flux and biomass heat storage flux are given in Barr et al. (2006). During the warm season when all components of the surface energy balance were resolved, the sum of the eddy-covariance sensible and latent heat fluxes

ACPD
15, 29265–29302, 2015

underestimated the surface available energy (net radiation minus surface storage) by ∼ 15 % (Barr et al., 2006).

2.2 Meteorology forcing data

The 30 min meteorological observations at 36 m height from OAS were used as atmospheric forcing data to drive Noah-MP in an uncoupled 1-D mode, including air temperature, specific humidity, wind speed, pressure, precipitation, downward solar, and longwave radiation. Figure 2 shows the annual mean temperature (1.5 °C) and total precipitation (406 mm) at this site during the study period (1998–2009). The most significant climatic features during the study period are a prolonged drought that began in July 2001 and extended throughout 2003, and an extended wet period from 2004–2007.

3 Methodology

3.1 The Noah-MP Model

Noah- MP is a new-generation of LSM, developed to improve major weaknesses of the Noah LSM (Chen et al., 1996; Chen and Dudhia, 2001). It is coupled to the WRF community weather and regional climate model (Barlage et al., 2015), and also available as a stand-alone 1-D model (Noah-MP v1.1). Noah-MP simulates several biophysical and hydrological processes that control fluxes between the surface and the atmosphere. These processes include surface energy exchange, radiation interactions with the vegetation canopy and the soil, hydrological processes within the canopy and the soil, a multi-layer snowpack, freeze-thaw, groundwater dynamics, stomatal conductance, and photosynthesis and ecosystem respiration. The major components include a 1-layer canopy, 3-layer snow, and 4-layer soil. Noah-MP provides a multi-parameterization framework that allows using the model with different combinations of alternative process schemes for individual processes (Niu et al., 2011). Alternative sub-modules for

ACPD
15, 29265–29302, 2015

12 physical processes can provide more than 5000 different combinations. Soil water fluxes are calculated by the Richards equation using a Campbell/Clapp-Hornberger parameterization of the hydraulic functions (Clapp and Hornberger, 1978). In the original version of Noah-MP, the vertical soil profile was treated as one mineral ground texture only.

3.2 Thermal and hydraulic parameterizations for organic soil

The OAS research site has an organic LFH (forest-floor) soil horizon, 8∼10 cm deep. This study evaluates the impact of adding an organic soil horizon in the Noah-MP model. The original Noah-MP soil parameterization included mineral soil horizons only. We added an organic soil horizon using a similar approach to Lawrence and Slater (2008), which parameterizes soil thermal and hydrologic properties in terms of carbon density in each soil layer. Soil carbon or organic fraction for each layer is determined as

$$f_{sc,i} = \frac{\rho_{sc,i}}{\rho_{sc,max}} \tag{1}$$

where $f_{sc,i}$ is the carbon fraction of the each layer, $\rho_{sc,i}$ is the soil carbon density, and $\rho_{sc,max}$ is the maximum possible value (peat density of 130 kg m^{-3}, Farouki, 1981). The soil properties for each layer are specified as a weighted combination of organic and mineral soil properties.

$$P = \left(1 - f_{sc,i}\right) P_m + f P_o \tag{2}$$

where P_m is the value for mineral soil, P_o is the value for organic soil, and P is the weighted average quantity. In this study, we assume that the top layer of the soil is made up of 100 % organic matter, consistent with the 8–10 cm LFH horizon at OAS. The remaining soil layers were assumed that made up of 100 % mineral soil. We have also conducted sensitive test for some key parameters, like Saturated hydraulic conductivity, porosity, Suction, Clapp and Hornberger parameter, following the work of Letts et al. (2000). The sensitivity test showed that the soil moisture is not very sensible to these parameters change, so we decided to use Lawrence and Slater (2008), Letts et al. (2000) recommended values instead, which are close enough to explain the observations (see Table 1).

3.3 Evaluation of model performance

Outputs from the Noah-MP simulations were evaluated against observations, using the Root Mean Squared Error (RMSE), square of the correlation coefficient (R^2), and Index of Agreement (IOA) (Zhang et al., 2013). The IOA is calculated as

$$\mathrm{IOA} = 1 - \frac{\sum_{i=1}^{N}(M_i - O_i)^2}{\sum_{i=1}^{N}(|O_i - O\overline{O}| + |M_i - \overline{O}|)^2} \tag{3}$$

where M_i and O_i are simulated and observed values of the same variable, respectively, and $\overline{O}$ is the mean of the observed values. IOA ranges from 0 (no agreement) to 1 (perfect match).

4 Model simulation

4.1 Noah-MP model Spin-up

The LSM spin-up is broadly defined as an adjustment processes as the model approaches its equilibrium following the initial anomalies in soil moisture content or after some abnormal environmental forcing (Yang et al., 1995). Without spin-up, the model results can be unstable and may exhibit drift as model states try to approach their equilibrium values. To initialize LSMs properly, the spin-up time required for LSMs to reach

ACPD
15, 29265–29302, 2015
The incorporation of an organic soil layer
L. Chen et al.

Title Page
Abstract Introduction
Conclusions References
Tables Figures
◀I ▶I
◀ ▶
Back Close
Full Screen / Esc
Printer-friendly Version
Interactive Discussion

the equilibrium stage needs to be examined first (Chen and Mitchell, 1999; Cosgrove et al., 2003). In this study, model runs for the year 1998 were performed repeatedly until all the soil-state variables reached the equilibrium state. The criterion that defines the equilibrium is when the difference between two consecutive one-year simulations becomes less than 0.1 % for the annual means (Cai et al., 2014; Yang et al., 1995). Yang et al. (1995) discussed the spin-up processes by comparing results from 22 LSMs for grass and forest sites, and showed a wide range of spin-up timescales (from 1 year to 20 years), depending on the model, state variable and vegetation type. Cosgrove et al. (2003) used four NLDAS-1 LSMs to discuss the spin-up time at selected six sub-regions covering North America, and showed that all models reached equilibrium between one to three years for all six sub-regions. In this study, we found that it requires 9 years for deep-soil moisture (100–200 cm layer) in Noah-MP to reach its equilibrium (Fig. 3), 8 years for latent heat flux and evapotranspiration, but only 3 years for the surface soil moisture. It takes a long time period to reach equilibrium especially in the deep soil layers. In OAS, the freezing/thawing is a relatively slow process, the "long-term" memory of the initial condition comparing to surface variables, so the freeze-thawing process makes the spin up slower. So we set 10 years for the spin-up time for all the experiments discussed here.

4.2 Sensitivity test of Noah-MP physics options

There are more than 5000 different combinations of physics parameterization schemes for the 12 sub-land processes in Noah-MP. We only selected the following critical processes to which our preliminary test results are sensitive: (1) CRS: canopy stomatal resistance, (2) BTR: soil moisture factor for stomatal resistance, (3) RUN: Runoff/soil lower boundary, (4) SFC: surface layer drag coefficient calculation, (5) FRZ: supercooled liquid water, (6) INF: soil permeability, and (7) RAD: radiative transfer. The options used in this study are listed in Table 2, with all possible combinations (1152) investigated. The impact of each parameterization option was investigated using two statistical indices and IOA. Table 3 shows the effect of each critical process, averaged

ACPD
15, 29265–29302, 2015

over all possible combinations of the other six processes (Gayler et al., 2014). The options that produced negative mean IOA values are ignored. For latent heat and sensible heat flux simulations, the scheme combinations generating good skill scores are the following: CRS (1), BTR (1), RUN (2), SFC (2), FRZ (1), INF (2), and RAD (3). They are then treated as the most appropriate combinations for our study site (see Table 3). The order of the categories based on the IOA scores from the highest to the lowest is SFC > FRZ > CRS > BTR > RUN > RAD > INF.

4.3 Evaluation results

We defined the combination of the parameterization schemes that produced the best performance in our simulation without incorporating organic soil as the "control experiment" (CTL); the simulation that used the same parameterization option combination but with the organic soil incorporated as the "organic layer experiment" (OGN).

We first evaluated the simulated CTL sensible and latent heat fluxes at the OAS site in relation to observations for the period of 1998–2009. Figure 4 show that the CTL run captures the observed monthly mean sensible heat and latent heat flux reasonably well. However, SH is underestimated in spring and slightly overestimated in summer. We then evaluated the Noah-MP model simulation with the organic-soil parameterization (Fig. 5). The OGN simulation shows similar characteristics to the CTL, with improved correlation coefficients between observations and simulations: increasing from 0.82 (CTL) to 0.89 (OGN) for SH and from 0.93 (CTL) to 0.97 (OGN) for LH. The OGN simulations also resolve the underestimation of SH in spring, but the overestimation in summer still remains. SH and LH show improvement of OGN over CTL, related to timing of soil thaw and warming in spring. CTL thaws the soil too early causing a premature rise in LH in spring (April and May) and an associated underestimation of spring SH. The spring (April–May) fluxes are much improved in the OGN parameterization. However, both OGN and CTL retain a serious positive bias in SH from June–September, especially for wet years.

Figure 6 shows good agreement between the observed and simulated monthly soil temperature for the OAS site. However, the effects of including an organic soil layer at the top (0–10 cm) on soil temperature are not uniform throughout the soil depth and year. The CTL and OGN simulations produced nearly identical shallow soil temperature. However, the OGN simulation substantially decreased deep soil temperatures (10–100 cm) in summer and slightly increased deep-layer soil temperature in winter, especially for the drought years 2002–2003, causing much improvement with the observations. The soil thawing period in spring is significantly affected by the OGN parameterization, the thermal conductivity of the organic horizon is much lower than that of the mineral soil, which delays the warming of the deep soil layers after snowmelt. In winter, the organic soil layer insulates the soil and results in relatively warmer wintertime soil temperatures for OGN compared with CTL. The difference is most pronounced in drought years (2002 and 2003) (Fig. 6) when the thinner snowpack provides less insulation. The less precipitation/snow leads to a stronger evaporation, and thus a reduction of heat conductivity. With an organic soil horizon, the lower soil water content in the topsoil layer (Fig. 7) reduces the heat loss through evaporation; the winter soil temperature then becomes significantly higher compared with CTL. This result is consistent with recent studies that show a simulated increase in winter soil temperature of up to 5 °C in boreal regions when including an organic layer (Koven et al., 2009; Rinke et al., 2008; Lawrence and Slater, 2008) in LSMs.

The inclusion of an organic soil horizon also affects the hydrologic cycle components such as soil water content, runoff, and evaporation (Fig. 7). For the top layer, the OGN parameterization increases the shallow soil water content in summer but decreases the liquid soil water content in winter, due to the contrasting water retention characteristics of organic and mineral soil. Note that the observed soil water content during wet years may be higher than the site means because the sensors were located in a low spot that is prone to flooding. This site got flooded in 2004 and the ground water has not dried since then, so that the soil was oversaturated during the period of 2004–2008. In the second soil layer, the observed soil water content was incorrect after the site

ACPD
15, 29265–29302, 2015

got flooded (2004–2008). With more precipitation for this wet period, the real soil water content should have a relatively high value. Since the OGN increases the soil water content, it should be more close to the true observation. From Fig. 7, it can be seen that the OGN improved the liquid water simulation in frozen-free periods, as the soil moisture data are not so unreliable when the soil is frozen and are therefore not very useful during the winter. So it is hard to evaluate which experiment is better in winter. In late spring when snow starts melting, both CTL and OGN simulate the same topsoil temperature (Fig. 6), with temperature increases to above the freezing point. It is clear that the soil liquid water content is mainly controlled by precipitation, soil hydraulic conductivity and runoff. The high porosity of organic soil in the topsoil layer helps to retain more snowmelt water and hence increases the topsoil layer liquid water content. For the deep soil layers, the soil liquid water content is highly influenced by the soil temperature. Liquid soil moisture increases during soil ice thawing period. The higher deep soil layer liquid water content in OGN than in CTL is mainly because that the soil hydraulic conductivity is higher for organic soil than mineral soil, so liquid water at first-layer can transport downward quickly into the deep layers. That is probably the reason although the organic soil layer is only added to the topsoil in this study, but it still can affect the deep layer due to the infiltration characteristics of the topsoil.

Simulated summer evaporation from the ground is smaller for OGN than CTL (Fig. 12). The water retention characteristics of the organic soil horizon favor both higher water retention and reduced evaporation, related to the high air-filled porosity of the organic soil at field capacity. The higher hydraulic conductivity of the organic soil allows the precipitation to be quickly transported downward from the topsoil layer to deep layers, leading to a relatively dry surface layer and less soil evaporation. The thermal conductivity is lower compared with that of the mineral soil, which then prevents deeper soil to warm up rapidly after snowmelt season. The lower thermal conductivity of the top organic soil affects the annual cycle of the ground heat flux. In summer the top layer is warmer than the deep layers, the ground heat flux then transfers heat downward. Because of the lower thermal conductivity of the organic soil, the total soil heat gained in

ACPD
15, 29265–29302, 2015

OGN is less than CTL. In winter, the organic soil layer insulates the deep soil from the cold atmosphere, resulting in a relatively higher wintertime soil temperature for OGN compared with the CTL simulation without organic layer. Because air temperature is lower than land surface temperature so heat is transferred upward from soil to the land surface, the lower thermal conductivity of the organic soil can prevent the soil to cool. On the other hand, the snowfall in winter may form a snow layer on the top of the soil, then the thermal conductivity of both organic and mineral soil become very close. This is maybe the reason why the OGN simulated soil temperature is only slightly increased in winter compared to CTL simulations. The OGN-CTL difference is strongest for the drought years 2001, 2002 and 2003. During these years, less precipitation/snow leads to stronger evaporation. With the organic soil layer on the top, the lower soil water content in the topsoil layer (Fig. 7) reduces the heat loss through evaporation; the winter soil temperature then becomes significantly higher compared with CTL experiment.

4.4 Impact of organic soil on diurnal cycle of surface energy and hydrology

In general, the OGN parameterization improved the simulation of daily daytime SH and LH in terms of both RMSE and IOA (Table 4), although the improvement was not apparent in the mean daily cycle. Compared with CTL, OGN increased IOA for both SH and LH, increased the bias in SH slightly by $\sim 6\,\%$, and decreased the bias in LH by $14\,\%$, (Table 4).

For the 12-year simulation period, the study site experienced a prolonged drought, beginning in July 2001 and extending throughout 2002 and 2003. We then choose year 2002 and 2003 to represent typical drought years, and year 2005 and 2006 to represent typical wet years (Fig. 2), to examine the effect of the organic soil under different climate conditions. For drought years (2002 and 2003), OGN increased daytime SH especially in spring, and slightly decreased SH at nighttime (Fig. 8). LH is well simulated by both OGN and CTL (Fig. 8), with OGN reducing daytime LH slightly. OGN overestimates daytime SH compared with observations, while CTL underestimates daytime SH for spring and summer (Fig. 8a, b) and slightly overestimates SH for autumn and winter

ACPD
15, 29265–29302, 2015

(Fig. 8c, d). OGN has a major impact on the daily cycle of soil temperature. Consistent with discussions in Sect. 4.3, the soil temperature below 10 cm simulated by OGN is lower in summer and higher in winter than that of the CTL simulation, and the OGN simulation has less bias than the CTL simulation. In OGN simulation, the soil hydraulic conductivity of the top soil layer is higher than CTL, the water moves faster into deep layers than in CTL simulation, the runoff then increases. Due to the high soil porosity of the organic soil, OGN simulation shows higher soil-ice fraction at the top soil layer during the freezing periods. The higher water capacity and higher soil-ice fraction of the organic soil then reduce liquid water content/soil moisture, these further lead to less evaporation (i.e., latent heat flux) during freezing periods (Spring), and a compensating increase of the sensible heat flux.

For wet years (Fig. 9), OGN produces in general higher daytime SH than CTL. For spring, OGN simulated SH agrees with the observation better than CTL, but it is similar to or slightly worse than CTL for other seasons. Simulated LH for both OGN and CTL agree with observations well, with a significant improvement by OGN in spring. Note that the OGN simulation also improves surface heat fluxes significantly in drought years, because the snowmelt process dominates during spring months. For other seasons, the OGN results are fairly close to CTL.

4.5 Impact of an organic soil horizon on annual cycle of surface energy and hydrology

In the last section, it is clear that the incorporation of the top organic layer helps improve the simulation of the diurnal cycle of the surface energy and hydrologic components in spring season. In the following, we focus on a detailed analysis of the annual cycle of the surface energy and hydrology variables for "dry" (Fig. 10) versus "wet" years (Fig. 11). Between June and September as shown in Fig. 10h, the upper two soil layers were unfrozen. The topsoil is wetter in OGN for both dry and wet years compared with CTL because organic soil can retain more water. As discussed in Sect. 4.3, for the deep soil layers, the liquid water content is influenced by the soil temperature and the movements of the soil liquid water content between soil layers. Since the soil hydraulic conductivity is higher for OGN than mineral soil, the water moves faster into deep soil layers than CTL, therefore the OGN simulate higher soil liquid water content in deep layers. The total soil column liquid water content keeps increasing before the soil temperature reaches above the freezing point (Figs. 10g, 11g), which is because the deep soil temperature is usually higher than the top soil so ice get melts earlier in deep layer.

By adding an organic soil layer, the soil ice content becomes higher due to higher porosity. For dry years, the impact of the organic soil on surface and sub-surface runoff is not significant (Fig. 10e, f). The increase in the summer latent heat flux and sensible heat flux are compensated by a decrease in soil heat flux, leading to a significant decrease in summer soil temperature. In winter, the latent and sensible heat fluxes are not modified by the organic soil, but increased soil heat flux leads to an increased soil temperature in winter. The most prominent change by adding organic soil layer is the partition between vegetation transpiration and direct ground evaporation (Fig. 12a and b) where the OGN simulation decreased ground surface evaporation.

For wet years (Fig. 11), the impact of the organic soil on surface and sub-surface runoff becomes more significant, especially for sub-surface runoff. The organic soil increases the surface runoff during the spring snowmelt season, and increases the sub-surface runoff throughout the year, because of the higher surface layer soil ice content and higher porosity. The sensible heat flux also increases significantly in spring, with an associated reduction in latent heat flux and soil heat flux. The summer soil temperature also decreases but in a less degree than that in dry years, because the soil heat flux deceases less compared with dry years. Unlike dry years, there is a significant runoff change in wet years, and the ground evaporation is also decreased (Fig. 12c and d). OGN produces more soil-ice content and higher soil porosity, and lead to higher deep-soil-layer water content than CTL simulations. In wet season, by adding an organic topsoil layer, the total column soil water increases due to the infiltration of the soil water into the deep soil. This then leads to an increase in the sub-surface

ACPD
15, 29265–29302, 2015

runoff. As the consequence, the volumetric liquid water becomes higher in summer for OGN compared with CTL simulation.

5 Summary and conclusions

In this study, the Noah-MP LSM was applied at the BERMS Old Aspen site to investigate the impact of adding a realistic organic soil horizon on simulated surface energy and water cycle components. This site has an about 8–10 cm deep organic forest-floor soil horizon, typical of boreal deciduous broadleaf forests. The selection of different parameterization schemes for each process within the current Noah-MP model significantly affected the simulation results. It is found that, based on the IOA scores from the highest to the lowest, the importance of physics parameterization scheme is SFC > FRZ > CRS > BTR > RUN > RAD > INF.

When including, for the first time, an organic-soil parameterization within the Noah-MP model, the verification results against site show significantly improved performance of the model in simulated surface energy fluxes. For instance, the simulated SH in spring were much improved, while in later summer the model overestimated those fluxes. Due to lower thermal conductivity, the OGN simulated soil temperature was decreased during summer and slightly increased during winter compared with the CTL simulation, and the OGN simulations were more consistent with observations and with previous studies (Lawrence and Slater, 2008). Also, due to higher porosity of the organic soil, the OGN simulation was able to retain more soil water content in summer. However, in winter, the OGN experiment produced less liquid soil-water content due to the lower temperature and higher porosity. Since most of the soil moisture is stored in soil ice, the liquid water content is reduced. However, the effects of including an organic soil layer on soil temperature are not uniform throughout the soil depth and year, and those effects are more prominent in summer and in deep soils.

For drought years, the OGN simulation substantially modified the partition between direct soil evaporation and vegetation transpiration. When water is limited in drought years, the OGN simulation significantly reduced the direct soil evaporation but still produced higher summer total evapotranspiration. Increased latent heat flux and sensible heat flux in summer in OGN are compensated by decreased soil heat flux, leading to reduced soil temperature in summer. For wet years, the OGN simulated latent heat fluxes are similar to CTL except for spring season where OGN produced less evaporation. The incorporation of an organic layer at the top of the soil helps improve the nighttime sensible heat flux for all seasons. In addition, the impact of the organic soil on sub-surface runoff is substantive with much higher runoff throughout the season.

This preliminary study explored the effects of incorporating organic soil parameterization in Noah-MP on surface energy and water cycle for one flux site in boreal forest area. Given important role of boreal forests in the regional climate system by reducing winter albedo and also acting as a carbon sink and water source to the atmosphere and differences in forest structures and soils in the general boreal ecosystem, further work is needed to evaluate the Noah-MP with organic-soil parameterization at regional scales. We plan to evaluate the performance of the offline Noah-MP model and Noah-MP coupled with WRF for a broad boreal forest region including Alberta and Saskatchewan.

Acknowledgements. The author Liang Chen acknowledge the support from the National Basic Research Program (Grant No. 2012CB956203) and National Natural Science Foundation of China (Grant No. 41305062). The authors Liang Chen, Yanping Li, Alan Barr gratefully acknowledge the support of this work from Global Institute of Water Security at University of Saskatchewan. Fei Chen, Michael Barlage and Bingcheng Wan appreciate the support from the Water System Program at the National Center for Atmospheric Research (NCAR), and NOAA MAPP-CTB grant (NA14OAR4310186). NCAR is sponsored by the National Science Foundation. Any opinions, findings, conclusions or recommendations expressed in this publication are those of the authors and do not necessarily reflect the views of the National Science Foundation.

References

Barlage, M., Tewari, M., Chen, F., Miguez-Macho, G., Yang, Z. L., and Niu, G. Y.: The effect of groundwater interaction in North American regional climate simulations with WRF/Noah-MP, Climatic Change, 129, 485–498, 2015.

Bartlett, P. A., McCaughey, J. H., Lafleur, P. M., and Verseghy, D. L.: A comparison of the mosaic and aggregated canopy frameworks for representing surface heterogeneity in the Canadian boreal forest using CLASS: A soil perspective, J. Hydrol., 266, 15–39, 2002.

Barr, A. G., Black, T. A., Hogg, E. H., Kljun, N., Morgenstern, K., and, Nesic Z.: Inter-annual variability in the leaf area index of a boreal aspen-hazelnut forest in relation to net ecosystem production, Agr. Forest Meteorol., 126, 237–255, 2004.

Barr, A. G., Morgenstern, K., Black, T. A., McCaughey, J. H., and Nesic, Z.: Surface energy balance closure by the eddy-covariance method above three boreal forest stands and implications for the measurement of the CO_2 flux, Agr. Forest Meteorol., 140, 322–337, 2006.

Beringer, J., Tapper, N. J., McHugh, I., Chapin, F., Lynch, A. H., Serreze, M. C., and Slater, A.: Impact of arctic treeline on synoptic climate, Geophys. Res. Lett., 28, 4247–4250, 2001.

Boelter, D. H.: Important physical properties of peat materials, Proceedings of the 3rd International Peat Congress, Quebec, 150–156, 1968.

Bonan, G. B.: Atmosphere-biosphere exchange of carbon dioxide in boreal forests, J. Geophys. Res., 96, 7301–7312, doi:10.1029/90JD02713, 1991.

Bonan, G. B.: Effects of land use on the climate of the United States, Climatic Change, 37, 449–486, 1997.

Bonan, G. B., Pollard, D., and Thompson, S. L.: Effects of Boreal Forest Vegetation on Global Climate, Nature, 359, 716–718, 1992.

Bryant, D., Nielsen, D., and Tangley, L.: The Last Frontier Forests: Ecosystems and Economies on the Edge, World Resources Institute, 1997.

Cai, X., Yang, Z. L., David, C. H., Niu, G. Y., and Rodell, M.: Hydrological evaluation of the Noah-MP land surface model for the Mississippi River Basin, J. Geophys. Res.-Atmos., 119, 23–38, 2014.

Chen, F. and Dudhia, J.: Coupling an advanced land surface-hydrology model with the Penn State-NCAR MM5 modeling system. Part I: Model implementation and sensitivity, Mon. Weather Rev., 129, 569–585, 2001.

Chen, F. and Mitchell, K.: Using GEWEX/ISLSCP forcing data to simulate global soil moisture fields and hydrological cycle for 1987–1988, J. Meteorol. Soc. Japan, 77, 1–16, 1999.
Chen, F., Mitchell, K., Schaake, J., Xue, Y., Pan, H. L., Koren, V., Duan, Q. Y., Ek, M., and Betts, A.: Modeling of land surface evaporation by four schemes and comparison with fife observations, J. Geophys. Res.-Atmos., 101, 7251–7268, 1996.
Chen, F., Barlage, M. J., Tewari, M., Rasmussen, R. M., Jin, J., Lettenmaier, D., Livneh, B., Lin, C., Miguez-Macho, G., Niu, G. Y., Wen, L., and Yang, Z. L.: Modeling seasonal snowpack evolution in the complex terrain and forested Colorado Headwaters region: A model intercomparison study, J. Geophys. Res.-Atmos., 119, 13795–13819, doi:10.1002/2014jd022167, 2014.
Ciais, P., Tans, P. P., Trolier, M., White, J. W. C., and Francey, R. J.: A large northern hemisphere terrestrial CO_2 sink indicated by the 13C/12C ratio of atmospheric CO_2, Science-New York then Washington, 1098–1098, 1995.
Clapp, R. B. and Hornberger, G. M.: Empirical equations for some soil hydraulic properties, Water Resour. Res., 14, 601–604, 1978.
Cosgrove, B. A., Lohmann, D., Mitchell, K. E., Houser, P. R., Wood, E. F., Schaake, J. C., Robock, A., Marshall, C., Sheffield, J., Duan, Q., Luo, L., Higgins, R. W., Pinker, R. T., Tarpley, J. D., and Meng, J.: Real-time and retrospective forcing in the North American Land Data Assimilation System (NLDAS) project, J. Geophys. Res., 108, 8842, doi:10.1029/2002JD003118, 2003.
Dai, Y., Zeng, X., Dickinson, R. E., Baker, I., Bonan, G. B., Bosilovich, M. G., Denning, A. S., Dirmeyer, P. A., Houser, P. R., Niu, G., Oleson, K. W., Schlosser, C. A., and Yang, Z.-L.: The common land model, B. Am. Meteorol. Soc., 84, 1013–1023, 2003.
Dickinson, R. E.: Biosphere/atmosphere transfer scheme (bats) for the ncar community climate model, Technical report, 1986.
Dingman, S. L.: Physical Hydrology, MacMillan Publishing Company, New York, 1994.
Ek, M. B., Mitchell, K. E., Lin, Y., Rogers, E., Grunmann, P., Koren, V., Gayno, G., and Tarpley, J. D.: Implementation of Noah land surface model advances in the National Centers for Environmental Prediction operational mesoscale Eta model, J. Geophys. Res.-Atmos., 108, 8851, doi:10.1029/2002JD003296, 2003.
Farouki, O. T.: Thermal properties of soils, Report No. Vol. 81, No. 1, CRREL Monograph, 1981.
Gayler, S., Wöhling, T., Grzeschik, M., Ingwersen, J., Wizemann, H. D., Warrach-Sagi, K., Högy, P., Attinger, S., Streck, T., and Wulfmeyer, V.: Incorporating dynamic root growth enhances

the performance of Noah-MP at two contrasting winter wheat field sites, Water Resour. Res., 50, 1337–1356, doi:10.1002/2013WR014634, 2014.

Koven, C. D., Friedlingstein, P., Ciais, P., Khvorostyanov, D., Krinner, G., and Tarnocai, C.: On the formation of high-latitude soil carbon stocks: Effects of cryoturbation and insulation by organic matter in a land surface model, Geophys. Res. Lett., 36, L21501, doi:10.1029/2009gl040150, 2009.

Lawrence, D. M. and Slater, A. G.: Incorporating organic soil into a global climate model, Clim. Dynam., 30, 145–160, 2009.

Letts, M. G., Roulet, N. T., Comer, N. T., Skarupa, M. R., and Verseghy, D. L.: Parametrization of peatland hydraulic properties for the Canadian land surface scheme, Atmos.-Ocean, 38, 141–160, 2000.

Levine, E. R. and Knox, R. G.: Modeling soil temperature and snow dynamics in northern forests, J. Geophys. Res., 102, 29407–29416, doi:10.1029/97JD01328, 1997.

Molders, N. and Romanovsky, V. E.: Long-term evaluation of the hydro- thermodynamic soil-vegetation scheme's frozen ground/permafrost component using observations at barrow, alaska, J. Geophys. Res.-Atmos., 111, D04105, doi:10.1029/2005JD005957, 2006.

Nicolsky, D., Romanovsky, V., Alexeev, V., and Lawrence, D.: Improved modeling of permafrost dynamics in a GCM land-surface scheme, Geophys. Res. Lett., 34, L08501, doi:10.1029/2007GL029525, 2007.

Niu, G. Y., Yang, Z. L., Mitchell, K. E., Chen, F., Ek, M. B., Barlage, M., Kumar, A., Manning, K., Niyogi, D., and Rosero, E.: The community Noah land surface model with multiparameterization options (Noah-MP): 1. Model description and evaluation with local-scale measurements, J. Geophys. Res.-Atmos., 116, D12109, doi:10.1029/2010JD015139, 2011.

Oleson, K. W., Niu, G.-Y., Yang, Z.-L., Lawrence, D. M., Thornton, P. E., Lawrence, P. J., Stöckli, R., Dickinson, R. E., Bonan, G. B., Levis, S., Dai, A., and Qian, T.: Improvements to the Community Land Model and their impact on the hydrological cycle, J. Geophys. Res., 113, G01021, doi:10.1029/2007JG000563, 2008.

Radforth, N. W. and Brawner, C. O.: Muskeg and the northern environment in Canada, in: Muskeg Research Conference 1973: Edmonton, Alberta, University of Toronto Press, 1977.

Rinke, A., Kuhry, P., and Dethloff, K.: Importance of a soil organic layer for Arctic climate: A sensitivity study with an Arctic RCM, Geophys. Res. Lett., 35, L13709, doi:10.1029/2008GL034052, 2008.

ACPD
15, 29265–29302, 2015

The incorporation of an organic soil layer

L. Chen et al.

Thomas, G. and Rowntree, P. R.: The Boreal Forests and Climate. Q. J. Roy. Meteorol. Soc., 118, 469–497, doi:10.1002/qj.49711850505, 1992.

Viterbo, P. and Betts, A. K.: Impact on ECMWF forecasts of changes to the albedo of the boreal forests in the presence of snow, J. Geophys. Res., 104, 27803–27810, doi:10.1029/1998JD200076, 1999.

Yang, Z. L., Dickinson, R. E., Henderson-Sellers, A., and Pitman, A. J.: Preliminary study of spin-up processes in land surface models with the first stage data of project for intercomparison of land surface parameterization schemes phase 1 (a), J. Geophys. Res.-Atmos., 100, 16553–16578, 1995.

Yang, Z. L., Niu, G. Y., Mitchell, K. E., Chen, F., Ek, M. B., Barlage, M., Longuevergne, L., Manning, K., Niyogi, D., and Tewari, M.: The community Noah land surface model with multiparameterization options (Noah-MP): 2. Evaluation over global river basins, J. Geophys. Res.-Atmos., 116, D12110, doi:10.1029/2010JD015140, 2011.

Zhang, G., Zhou, G., Chen, F., Barlage, M., and Xue, L.: A trial to improve surface heat exchange simulation through sensitivity experiments over a desert steppe site, J. Hydrometeor, 15, 664–684, doi:10.1175/jhm-d-13-0113.1, 2014.

ACPD
15, 29265–29302, 2015

Table 1. Soil parameters used in Noah-MP for mineral soil texture classes (SANDY CLAY LOAM) and organic soil.

Soil Type	λ_s ($\mathrm{w\,m^{-1}\,K^{-1}}$)	λ_{sat} ($\mathrm{w\,m^{-1}\,K^{-1}}$)	λ_{dry} ($\mathrm{w\,m^{-1}\,K^{-1}}$)	c_s ($\mathrm{J\,m^{-3}\,K^{-1}} \times 10^6$)	θ_{sat}	κ_{sat}	ψ_{sat}	b
Mineral	6.04	2.24	0.23	2.0	0.421	0.00445	−135	6.77
Organic	0.25	0.55	0.05	2.5	0.9	0.100	−10.3	2.7

The soil parameters are λ_s is the thermal conductivity of soil solids, λ_{sat} is the unfrozen saturated thermal conductivity, λ_{dry} is the dry soil thermal conductivity, c_s is the soil solid heat capacity, θ_{sat} is the saturated volumetric water content (porosity), κ_{sat} is the saturate hydraulic conductivity, ψ_{sat} is the saturated matric potential, and b is the Clapp and Hornberger parameter.

ACPD
15, 29265–29302, 2015

The incorporation of an organic soil layer

L. Chen et al.

Table 2. Noah-MP options investigated in this Study.

Process	Options
CRS: Canopy stomatal resistance	= 1 : BALL-Berry = 2 : Jarvis
BTR: Soil moisture factor for stomatal resistance	= 1 : Noah = 2 : CLM = 3 : SSiB
RUN: Runoff/soil lower boundary	= 1 : TOPMODEL with ground water (Niu et al., 2007) = 2 : TOPMODEL with equilibrium water table (Niu et al., 2005) = 3 : original surface and subsurface runoff (free drainage) = 4 : BATS surface and subsurface runoff (free drainage)
SFC: Surface layer drag Coefficient calculation	= 1 : Monin-Obukhov = 2 : original Noah = 3 : MYJ consistent = 4 : YSU consistent
FRZ: Supercooled liquid water	= 1 : no iteration (Niu and Yang, 2006) = 2 : Koren's iteration
INF: Soil permeability	= 1 : linear effects, more permeable (Niu and Yang, 2006) = 2 : nonlinear effects, less permeable (old)
RAD: Radiative transfer	= 1 : modified two-stream = 2 : two-stream applied to grid-cell = 3 : two-stream applied to vegetated fraction

ACPD
15, 29265–29302, 2015

Table 3. Averaged statistical indices for SH and LH to the observations (R^2: correlation coefficient square; RMSE: root mean square error; IOA: index of agreement).

Options		SH			LH		
		R^2	RMSE	IOA	R^2	RMSE	IOA
CRS	1	0.703	76.648	0.805	0.659	47.099	0.869
	2	0.663	77.821	0.795	0.606	53.028	0.852
BTR	1	0.696	76.154	0.804	0.651	47.872	0.869
	2	0.683	77.383	0.801	0.629	50.496	0.854
	3	0.669	78.166	0.795	0.618	51.823	0.859
RUN	1	0.696	75.099	0.801	0.702	45.525	0.904
	2	0.700	74.518	0.802	0.718	44.050	0.913
	3	0.668	79.455	0.798	0.564	54.774	0.822
	4	0.668	79.866	0.799	0.546	55.906	0.803
SFC	1	0.707	74.134	0.890	0.667	48.736	0.871
	2	0.693	63.124	0.880	0.681	47.496	0.883
	3	–	–	–	–	–	–
	4	0.649	94.445	0.630	0.550	53.959	0.829
FRZ	1	0.688	75.193	0.795	0.728	44.341	0.916
	2	0.678	79.276	0.806	0.537	55.787	0.805
INF	1	0.683	77.291	0.800	0.632	50.147	0.860
	2	0.683	77.177	0.800	0.633	49.981	0.862
RAD	1	0.683	77.135	0.799	0.635	49.872	0.861
	2	0.682	77.396	0.802	0.628	50.455	0.860
	3	0.684	77.171	0.799	0.635	49.865	0.861

ACPD
15, 29265–29302, 2015

Table 4. Averaged statistical indices for CTL and OGN simulated SH and LH compared with the observations for each year [daytime, 08:00–16:00 local time (LT)] (R^2: correlation coefficient square; RMSE: root mean square error; IOA: index of agreement).

Year	SH						LH					
	CTL			OGN			CTL			OGN		
	R^2	RMSE	IOA	R^2	RMSE	IOA	R^2	RMSE	IOA	R^2	RMSE	IOA
1998	0.57	77.58	0.84	0.68	81.48	0.85	0.72	50.76	0.92	0.80	43.10	0.94
1999	0.62	62.22	0.88	0.73	69.45	0.88	0.72	46.26	0.92	0.81	37.73	0.95
2000	0.62	68.17	0.88	0.72	74.00	0.88	0.70	47.34	0.91	0.76	43.45	0.92
2001	0.74	58.82	0.91	0.80	65.40	0.91	0.79	38.55	0.94	0.85	32.84	0.96
2002	0.76	65.97	0.92	0.78	69.48	0.92	0.71	35.84	0.91	0.73	37.17	0.92
2003	0.77	55.61	0.93	0.79	56.11	0.94	0.70	37.38	0.91	0.73	41.28	0.90
2004	0.71	61.82	0.91	0.77	63.95	0.92	0.74	40.08	0.92	0.78	36.79	0.94
2005	0.64	62.84	0.89	0.79	61.24	0.92	0.69	49.36	0.91	0.82	34.61	0.95
2006	0.56	68.50	0.85	0.71	70.91	0.88	0.72	54.23	0.92	0.85	41.14	0.95
2007	0.63	64.78	0.88	0.75	66.14	0.91	0.73	51.66	0.92	0.84	38.35	0.95
2008	0.71	60.46	0.91	0.78	68.51	0.91	0.73	47.69	0.92	0.85	36.07	0.96
2009	0.70	62.83	0.90	0.76	68.13	0.91	0.76	40.79	0.93	0.81	36.57	0.95

ACPD
15, 29265–29302, 2015

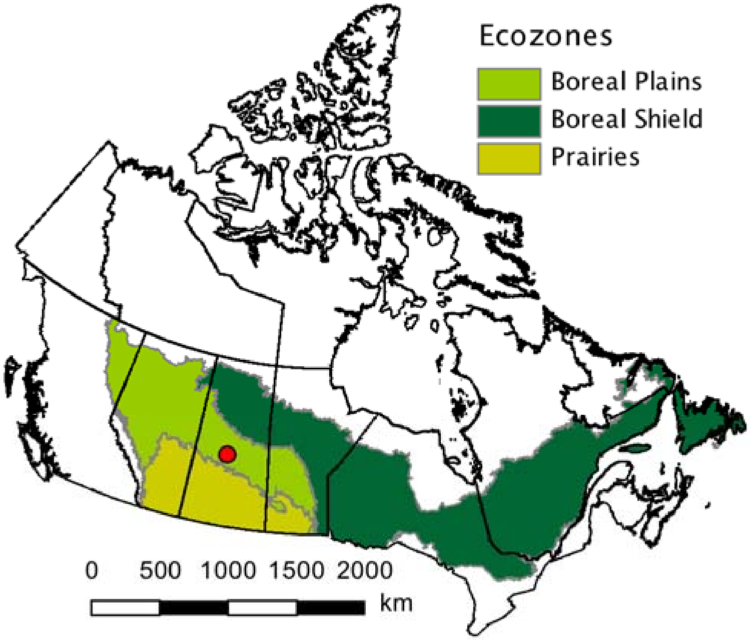

Figure 1. The location of the study site (Old Aspen Flux Tower).

ACPD
15, 29265–29302, 2015

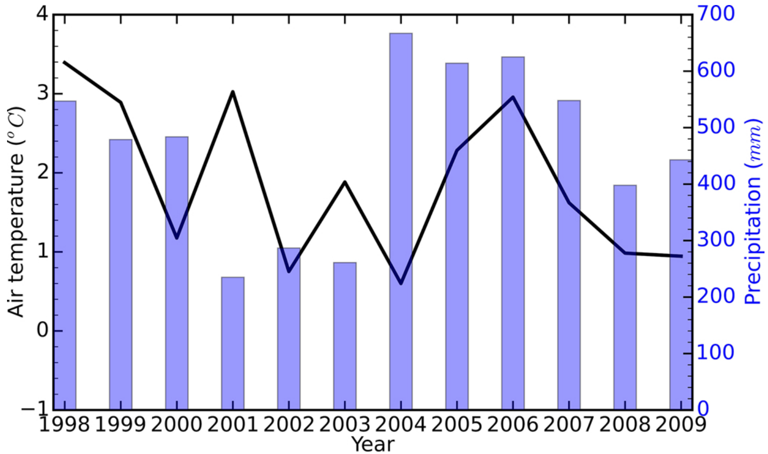

Figure 2. Monthly air temperature above canopy and precipitation at BERMS SK-OAS site.

ACPD
15, 29265–29302, 2015

Title Page
Abstract | Introduction
Conclusions | References
Tables | Figures
◀| |▶
◀ ▶
Back | Close
Full Screen / Esc
Printer-friendly Version
Interactive Discussion

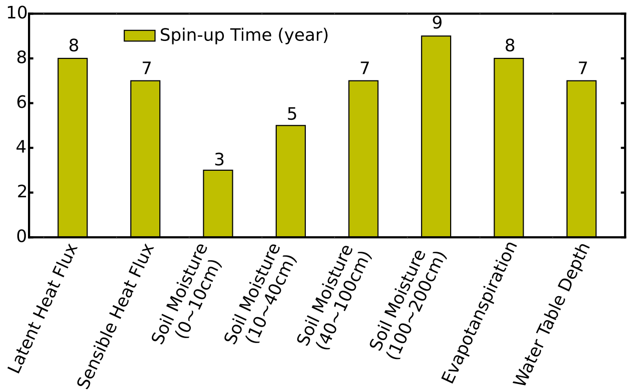

Figure 3. Averaged spin-up time (in years) for individual variables.

ACPD
15, 29265–29302, 2015

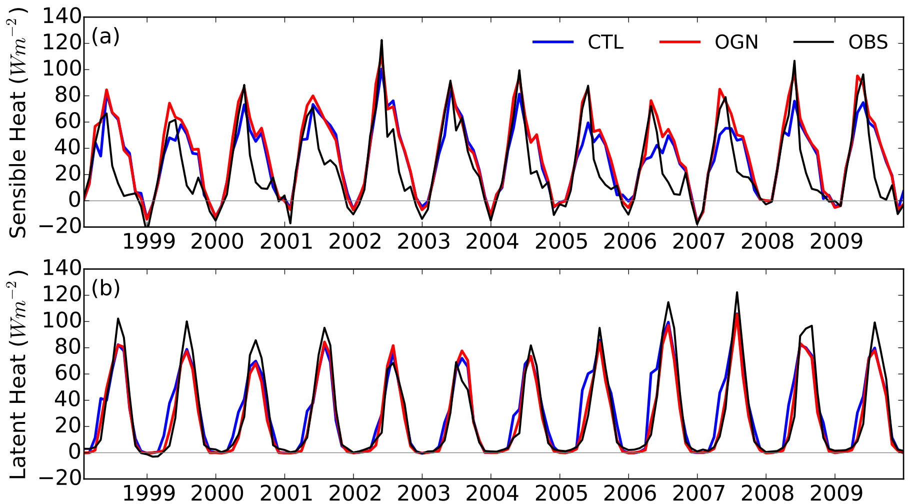

Figure 4. Comparison of the observed and the Noah-MP simulated (CTL and OGN) sensible and latent heat flux above canopy.

ACPD
15, 29265–29302, 2015

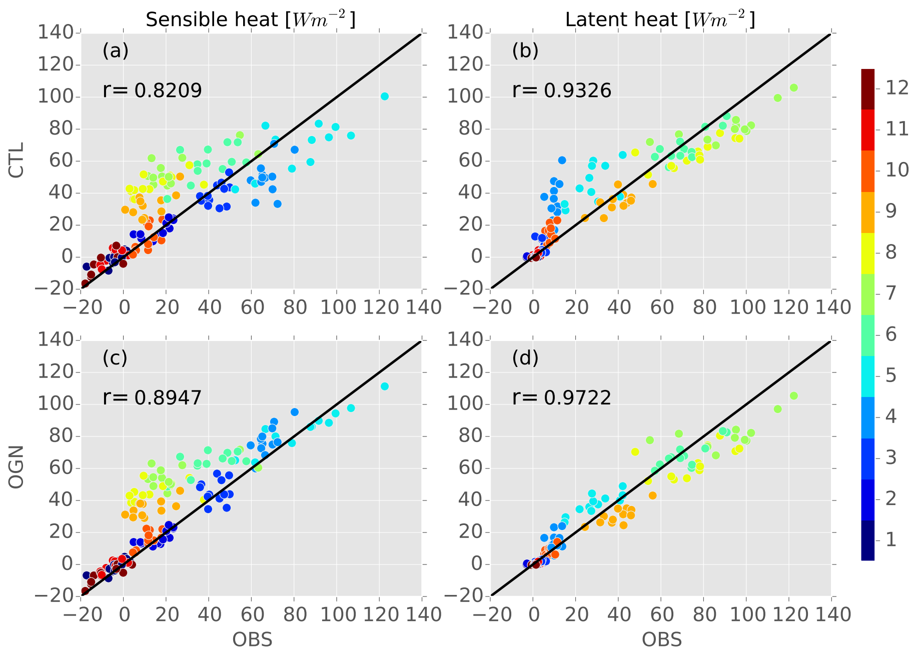

Figure 5. Scatterplots of the monthly-averaged **(a)** sensible, **(b)** latent heat fluxes ($\mathrm{W\,m^{-2}}$) for CTL versus the observation above canopy; the monthly-averaged **(c)** sensible, **(d)** latent heat fluxes ($\mathrm{W\,m^{-2}}$) for OGN versus the observation above canopy.

ACPD
15, 29265–29302, 2015

Title Page
Abstract | Introduction
Conclusions | References
Tables | Figures
◂◂ | ▸▸
◂ | ▸
Back | Close
Full Screen / Esc
Printer-friendly Version
Interactive Discussion

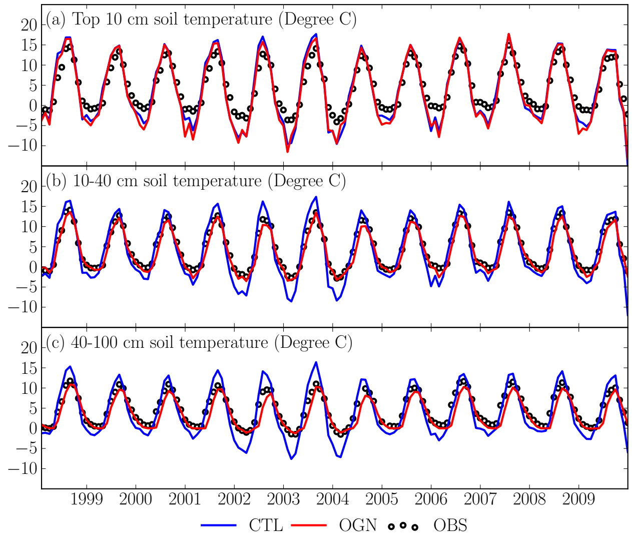

Figure 6. Observed and Noah-MP-simulated monthly soil temperature for BERMS SK-OAS site at a depth of **(a)** top 10 cm, **(b)** 10–40 cm, and **(c)** 40–100 cm.

ACPD
15, 29265–29302, 2015

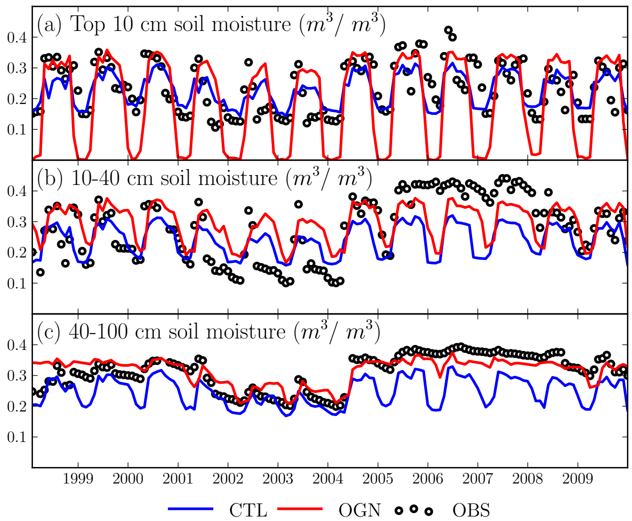

Figure 7. Observed and Noah-MP-simulated monthly soil moisture for BERMS SK-OAS site at a depth of **(a)** top 10 cm, **(b)** 10–40 cm, and **(c)** 40–100 cm.

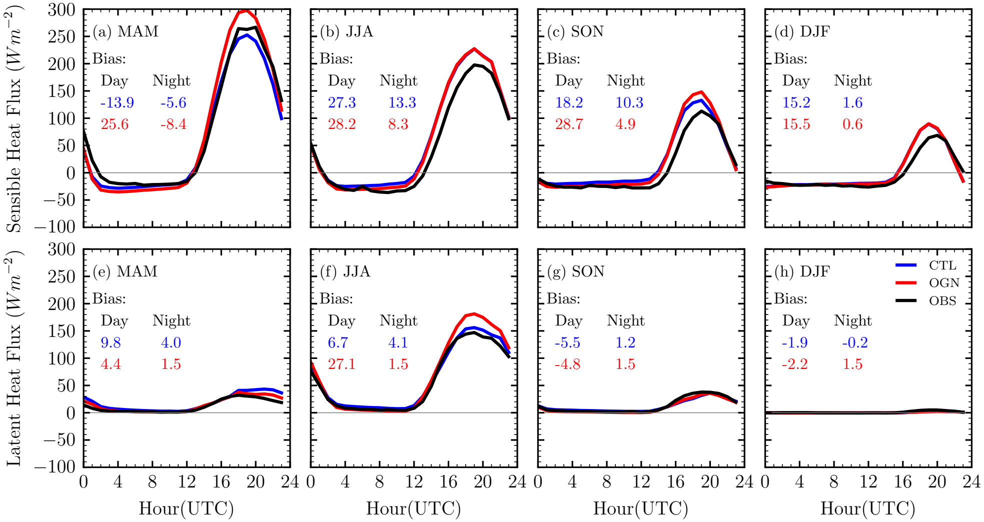

Figure 8. Comparison of the seasonal averaged diurnal cycle of the sensible and latent heat fluxes at OAS site for drought years.

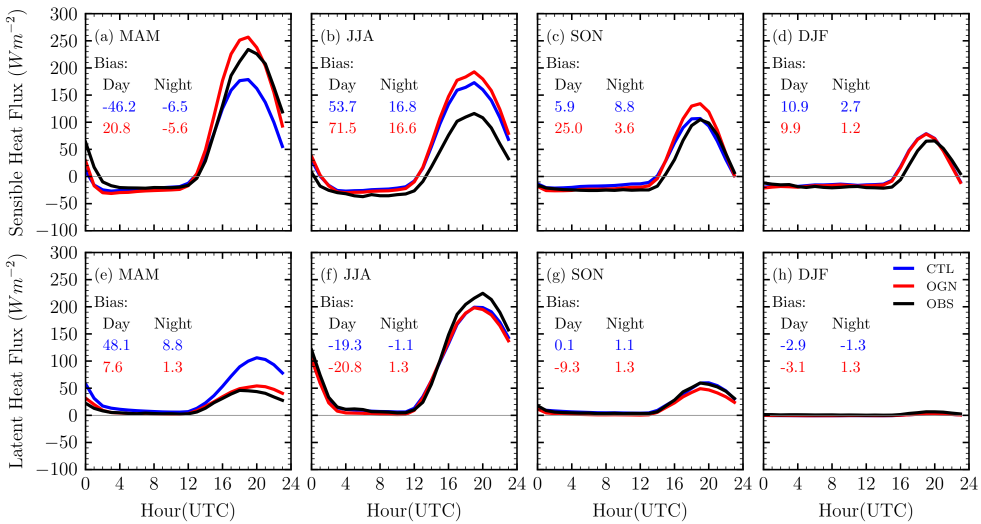

Figure 9. Comparison of the seasonal averaged diurnal cycle of the sensible and latent heat fluxes at OAS site for wet years.

ACPD
15, 29265–29302, 2015

The incorporation of an organic soil layer

L. Chen et al.

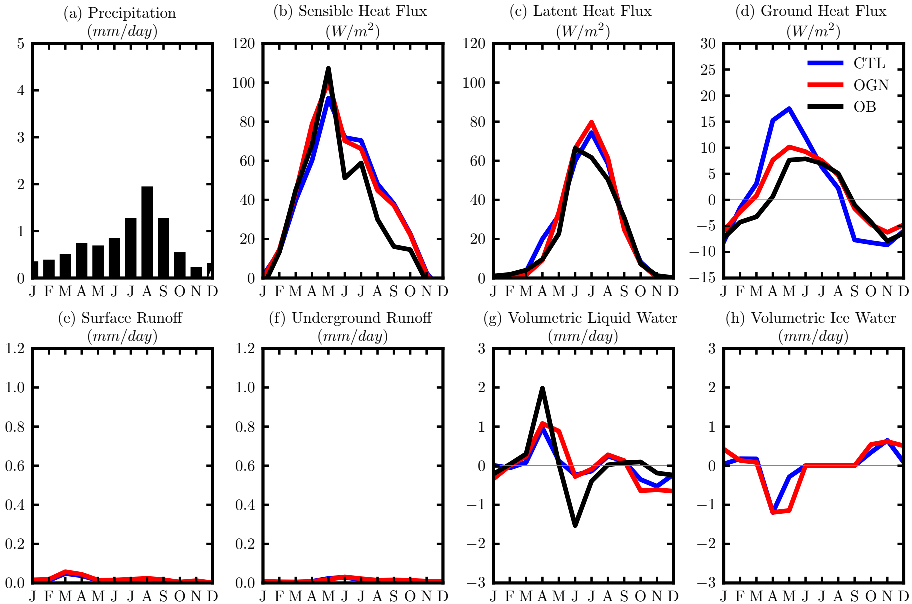

Figure 10. Annual cycle of selected surface energy and hydrologic cycle fields for drought years. Black line is the observation. Black line is the observation. Note that **(a)** is the observed precipitation, **(b)** is sensible heat flux, **(c)** is latent heat flux, **(d)** is ground heat flux, **(e)** is surface runoff, **(f)** is underground runoff, **(g)** is the total column soil liquid water content changes, **(h)** is the total column soil ice water content changes.

ACPD
15, 29265–29302, 2015

Title Page
Abstract | Introduction
Conclusions | References
Tables | Figures
◀▮ | ▶▮
◀ | ▶
Back | Close
Full Screen / Esc
Printer-friendly Version
Interactive Discussion

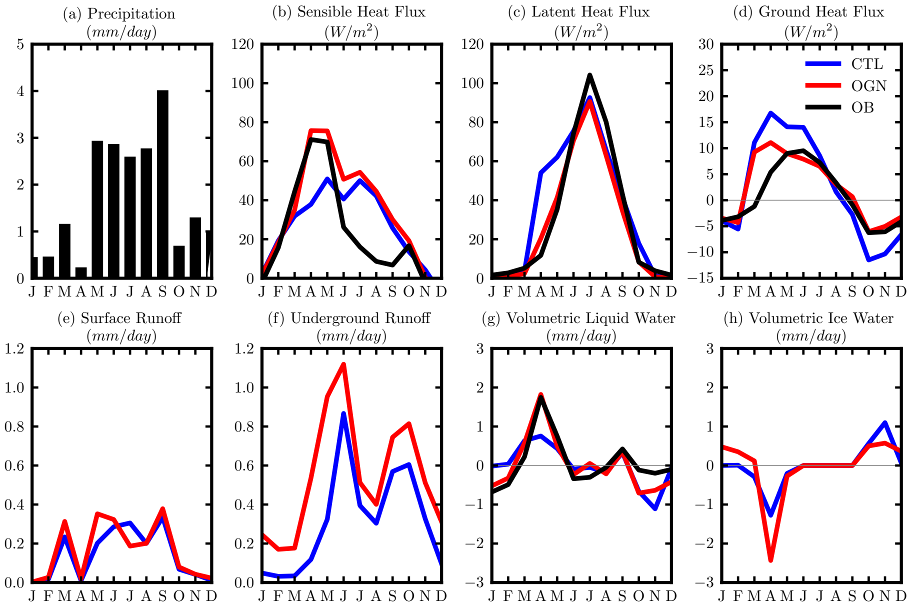

Figure 11. Annual cycle of selected surface energy and hydrologic cycle fields for wet years. Black line is the observation. Note that **(a)** is the observed precipitation, **(b)** is sensible heat flux, **(c)** is latent heat flux, **(d)** is ground heat flux, **(e)** is surface runoff, **(f)** is underground runoff, **(g)** is the total column soil liquid water content changes, **(h)** is the total column soil ice water

ACPD

15, 29265–29302, 2015

The incorporation of an organic soil layer

L. Chen et al.

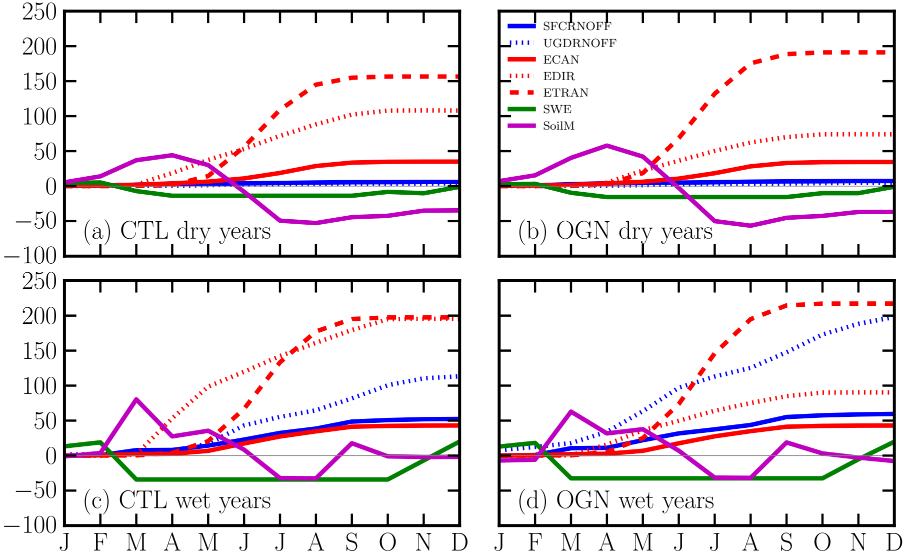

Figure 12. Water budgets: blue lines are accumulated surface runoff (mm), blue dots are accumulated underground runoff (mm), red lines are accumulated evaporation of intercepted water (mm), red dots are accumulated ground surface evaporation (mm), red dash lines are accumulated transpiration (mm), green lines are snow water equivalent changes (mm), purple lines are soil water content changes in the soil column (mm), **(a)** and **(b)** are averaged for 2002–2003, **(c)** and **(d)** are averaged for 2005–2006.

ACPD

15, 29265–29302, 2015

The incorporation of an organic soil layer

L. Chen et al.